Increased Expression of Neuronal Apolipoprotein E in Human Brain With Cerebral Infarction

Kazuko Aoki, MD, PhD; Toshiki Uchihara, MD, PhD; Nobuo Sanjo, MD, PhD; Ayako Nakamura; Kenji Ikeda, MD, PhD; Kuniaki Tsuchiya, MD, PhD; Yoshihiro Wakayama, MD, PhD

Background and Purpose—Cellular origin of apolipoprotein E (ApoE) in the human brain and its roles in physiological and pathological conditions remain to be clarified.

Methods—Immunolocalization of ApoE was investigated in a series of autopsied human brains with or without infarction. ApoE expression was also estimated on immunoblot on protein extracts from autopsied brains and a cultured neuroblastoma cell line of human origin (GOTO) subjected to an oxidative stress induced by exposure to hydrogen peroxide (0.2 mmol/L).

Results—In addition to astrocytes and microglia, neurons and degenerated axons in and around the ischemic foci contained ApoE-like immunoreactivity, which was more intense in recent ischemic foci. Immunoblot demonstrated an increase in expression of ApoE in brain extracts from ischemic lesion, and this increase was also pronounced in the cultured neuroblastoma cell line after the stress.

Conclusions—Accumulation of ApoE in neurons in and around ischemic foci of the human brain is related to an increase in ApoE synthesis in neurons, as seen in cultured neuronal cells after oxidative stress. Intrinsic regenerative activity of neuron in reaction to external insults may be related to this increase in ApoE of neuronal origin. (***Stroke***. **2003;34:875-880.**)

Key Words: apolipoproteins ■ cerebral infarction ■ neurons ■ oxidative stress

Apolipoprotein E (ApoE) is synthesized in various organs, including liver, spleen, kidney, and brain, and is supposed to play multiple roles. There is accumulating evidence that ApoE in the central nervous system is involved not only in stable physiological conditions but also in more dynamic situations such as development, remodeling, degeneration, and regeneration.[1-6] Moreover, the cellular source of ApoE in the central nervous system, initially considered to be restricted to astrocytes,[7,8] is currently considered to be more variable according to conditions.[9-14]

In this study we attempted to examine the manner in which ApoE is expressed in human brain with ischemic foci to clarify how an insult to the central nervous system modifies the expression of ApoE, which has been reported to play certain roles in repair of the central nervous system.[1,15-17] A parallel in vitro study on a cultured cell line corroborated these in vivo findings.[18,19]

Methods

Autopsied brains from 9 patients with cerebral infarction, 6 patients with Alzheimer disease (AD), and 8 patients without neurological disorders were enrolled in this study. Clinical data of the patients are summarized in the Table. The time from the onset of the ischemic attack to death was between 8 days and 10 months, determined from the clinical records.

Immunohistochemistry

Formalin-fixed, paraffin-embedded blocks, including both the area of ischemic necrosis and the surrounding nonnecrotic area, were obtained at 10-μm thickness. Sections were deparaffinized and treated with a microwave oven in citrate buffer 3 times for 5 minutes, treated with 1% hydrogen peroxide for 30 minutes, then incubated for 3 days at 4°C with either ApoEC (1:2000; anti-human ApoE polyclonal antibody raised against a synthetic peptide EKVQAAVGTSAAPVPSDNH equivalent to the C-terminal amino acid sequence 299 to 317 of human apolipoprotein E; IBL) or ApoEAB947[20] (1:2000; anti-human recombinant ApoE; Chemicon) diluted with PBS containing 0.03% Triton-X 100 and the corresponding blocking serum. The sections were then incubated for 2 hours with a biotinylated secondary antibody (1:1000; Vector), followed by avidin-biotin-peroxidase complex (1:1000; ABC Elite, Vector). The peroxidase labeling was visualized with diaminobenzidine as chromogen, which yielded a brown reaction product after approximately 40 minutes, and then the stained sections were counterstained with hematoxylin.

Received November 8, 2001; final revision received November 11, 2002; accepted November 13, 2002.

From the Department of Neuropathology, Tokyo Metropolitan Institute for Neuroscience (K.A., T.U., N.S., A.N.), Tokyo; Department of Neurology, Fujigaoka Hospital of Showa University (K.A., Y.W.), Yokohama; Department of Neurology, Saitama Rehabilitation Center (N.S.), Saitama; Department of Neuropathology, Tokyo Institute of Psychiatry (K.I., K.T.), Tokyo; and Department of Laboratory Medicine and Pathology, Tokyo Metropolitan Matsuzawa Hospital (K.T.), Tokyo, Japan.

Correspondence to T. Uchihara, MD, PhD, Department of Neuropathology, Tokyo Metropolitan Institute for Neuroscience, 2-6 Musashi-dai, Fuchu, Tokyo, 183-8526 Japan. E-mail uchihara@tmin.ac.jp

Stroke is available at http://www.strokeaha.org

DOI: 10.1161/01.STR.0000064320.73388.C6

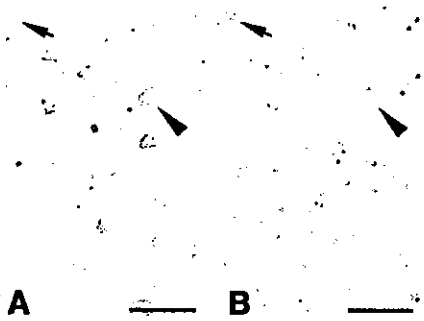

Figure 1. Immunostaining with ApoEC at the periphery of an ischemic focus counterstained with hematoxylin (bars=50 μm). A, Neurons exhibit ApoE-like immunoreactivity. B, ApoE-like immunoreactivity was completely abolished when ApoEC was coincubated with the antigen peptide. The same area as A in the adjacent section is shown, evidenced by the presence of the same blood vessel (arrow) and neurons (arrowhead).

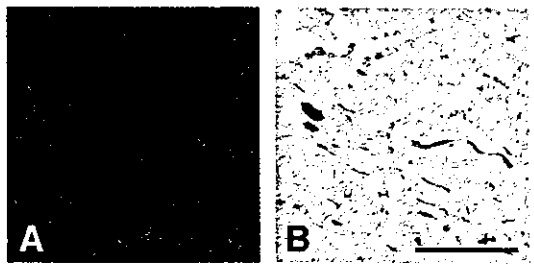

Figure 3. Accumulation of ApoE in degenerated axons (bar=50 μm). Colocalization of neurofilament epitope (A; labeling with SMI31 and visualized with FITC) and ApoE-like immunoreactivity (B; labeling with ApoEC and visualized with avidin-biotin-peroxidase method on the same section as A) confirmed axonal accumulation of ApoE.

results as ApoEC. This ApoE-like immunoreactivity in neurons was more pronounced in recent foci than in older foci. None of these neurons were atrophic or ischemic.

Double-labeled sections of ischemic foci demonstrated that ApoE-like immunoreactivity was present variably in neurons, some ballooned neurons (Figure 2A), astrocytes (Figure 2B), and microglia (Figure 2C). Double-labeling immunohistochemistry with anti-neurofilament (SMI-31; Figure 3A) and ApoEC (Figure 3B) antibodies clarified colocalization of these 2 epitopes, which confirmed that accumulation of ApoE was also extended into axons. ApoE-positive glial cells were, however, rarely observed where ApoE accumulated in neurons or axons and vice versa: neurons and axons immunopositive for ApoE were rarely in close contact with glial cells containing ApoE-like immunoreactivity (Figures 1 to 3).

Differences in immunolocalization of ApoE and in its immunoreactivity according to pathological conditions are shown in Figure 4. In control brains, ApoE-like immunoreactivity was at most faint in neurons (Figure 4A) or in subpial astroglia. In AD brains, ApoE-like immunoreactivity was accumulated in senile plaques and neurofibrillary tangles (Figure 4B), while other neuronal labeling was not comparable to that seen at the periphery of an ischemic focus (Figure 4C). Comparison of the ischemic area (Figure 4D, left) and its adjacent less affected area (Figure 4D, right) demonstrated that ApoE-like immunoreactivity in neurons was apparently more intense in areas involved in the ischemic process. Even in brains with ischemic focus, ApoE-like immunoreactivity in neurons was barely detectable in intact areas closely adjacent to the ischemic focus (Figure 4D).

Western Blot Analyses

Probing human brain extracts with ApoEC on Western blot demonstrated a major band at approximately 36 kDa (Figure 5A), as was detected similarly when probed with ApoEAB947. Quantitative analysis of the relative intensity of ApoE-immunoreactive bands (Figure 5B) demonstrated that expression of ApoE protein was significantly increased (P=0.0498, nonparametric method of Kruskal-Wallis) in AD brains (214%, mean relative to mean of controls, indicated as 1; P=0.0320, ANOVA) and further increased in brains with infarction (247%, mean relative to mean of controls; P=0.0132, ANOVA).

Probing extracts from human neuroblastoma cell line (GOTO) with ApoEC visualized bands similar to those seen in human brains (Figure 6A). Four independent sessions were followed up to 48 hours after exposure to hydrogen peroxide, and the density of ApoE-immunoreactive bands was quantified relative to the baseline (0 hours) of each session, indicated as 1 (Figure 6B). Quantitative analysis of the relative intensity of ApoE-immunoreactive bands demonstrated that expression of ApoE protein was dependent on intervals (P=0.0088, nonparametric method of Kruskal-

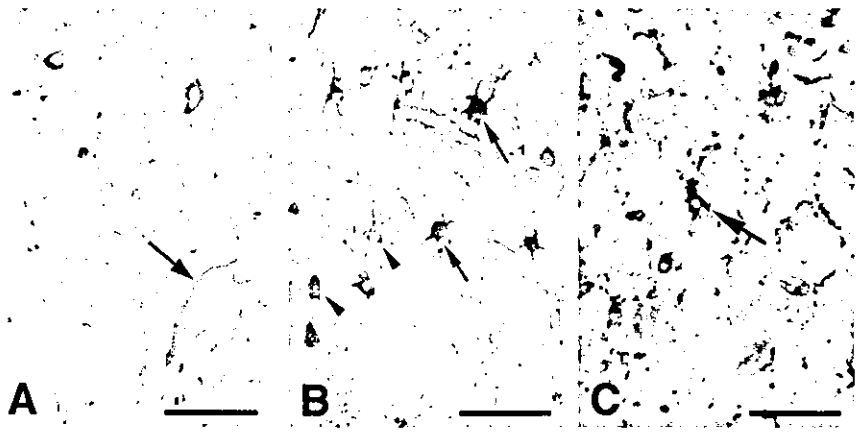

Figure 2. Cellular localization of ApoE around ischemic foci. A, Double immunolabeling of ApoEC (purple) and carbindin (brown) at the boundary of an ischemic focus. ApoE-like immunoreactivity is variable in each neuron, including a ballooned neuron (arrow; bar=50 μm). B, Double immunolabeling of GFAP (purple) and ApoEC (brown) at the boundary of an ischemic focus. In addition to double-stained astrocytes (arrows), intense ApoE-like immunoreactivity is present in neuronal cells (arrowheads; bar=50 μm). C, Double immunolabeling of RCA-120 (purple) and ApoEC (brown) at the boundary of ischemic foci. Some microglial cells (arrow) are ApoE immunopositive (bar=50 μm).

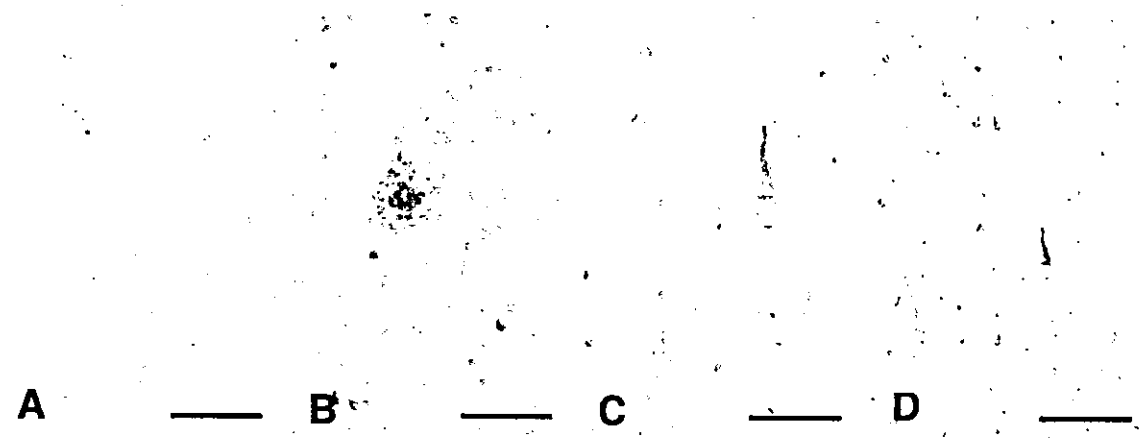

Figure 4. ApoE-like immunoreactivity (probed with ApoEC) in various pathological conditions (counterstained with hematoxylin). A, Control. Some neurons exhibit ApoE-like immunoreactivity, although it is at most very faint (bar=50 μm). B, AD. ApoE-like immunoreactivity is accumulated in senile plaques, while neuronal labeling is absent outside neurofibrillary tangles (bar=50 μm). C, At the periphery of an ischemic focus. ApoE-like immunoreactivity is intense in neurons (bar=50 μm). D, Low-power view of C. ApoE-immunoreactive neurons are abundant in the affected area (left), while they are absent in less affected area (right; bar=100 μm).

Wallis) after exposure to hydrogen peroxide. It increased at 4 hours (133%, mean relative to mean before exposure; $P=0.0213$, ANOVA). At 24 hours, this increase was more significant (168%; $P=0.0002$, ANOVA), which was progressive up to 48 hours (187%; $P=0.0002$, ANOVA). A consistent amount of β-actin immunoreactivity is seen at the bottom of Figure 5A and Figure 6A, suggesting that the amount of loaded protein was consistent.

Discussion

The major cellular source of ApoE in the brain has been considered to be astrocytes.[7,8] On the other hand, immunolocalization of ApoE to other cellular components, such as neurons in the hippocampus or frontal cortex, microglia, oligodendrocytes, and blood vessels, has also been reported.[9–14] It still remains to be clarified how ApoE is produced and handled in the brain. Moreover, little is known regarding how the metabolism of ApoE is altered in diseased brains. In the present study immunohistochemical investigation on human autopsied brains with ischemic lesions demonstrated that astrocytes and microglia contained ApoE-like immunoreactivity, as reported previously.[11,13] In addition to these glial components, neocortical neurons around the ischemic foci also contained abundant ApoE-like immunoreactivity. At least 2 possibilities have been proposed regarding the cellular source of ApoE in neurons. Because ApoE could be internalized through several receptors on plasma membrane,[19] it is speculated that ApoE in neurons is derived from astrocytes and is internalized through these carrier molecules.[1,23] Another possibility is that ApoE is produced in neurons, as demonstrated previously by in situ hybridization.[24] Although these 2 pathways are not mutually exclusive, the present study demonstrated that neurons were one of the major sites of ApoE synthesis in ischemic foci, in addition to glial cells. The absence of ApoE-positive glial cells around ApoE-positive neurons in ischemic foci suggests that ApoE is synthesized in these neurons and is not derived exogenously. Moreover, accumulation of ApoE was not only restricted to neuronal soma but also extended into degenerated axons (Figure 3B), again not in contact with ApoE-positive glial cells, which suggests a neuronal origin of ApoE. Although it has been reported that some neurons without disease possibly exhibit ApoE-like immunoreactivity in human brain,[12,25] it was at most faint in the present study. Because the same antibody visualized a significant amount of ApoE on Western blot (Figure 5A), it is likely that sampling, routine fixation in formalin, and processing in paraffin, as used in the present study, might have attenuated immunohistochemical labeling of ApoE in normal neurons. Fixation with another fixative (such as paraformaldehyde) and use of free-floating sections

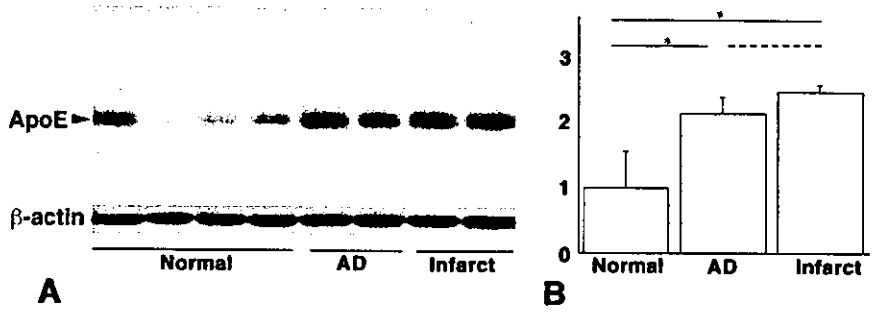

Figure 5. Western blot of extracts from human brains probed with ApoEC (A) and its densitometric quantification (B). A, ApoEC-immunoreactive bands at approximately 36 kDa, derived from brains with infarction (Infarct) and from those with AD, are more intense than those from normal brains (Normal). Arrowhead: 36 kDa. β-Actin–immunoreactive bands are shown as an internal control (bottom). B, Relative intensity of ApoEC-immunoreactive bands (mean±SD) was quantified and expressed with mean of normal brains (n=4) as a reference, indicated as 1. ApoE-immunoreactive bands are more intense in AD brains (n=2) and in brains with infarction (n=2) relative to normal brains. *$P<0.05$; broken line indicates not significant by ANOVA.

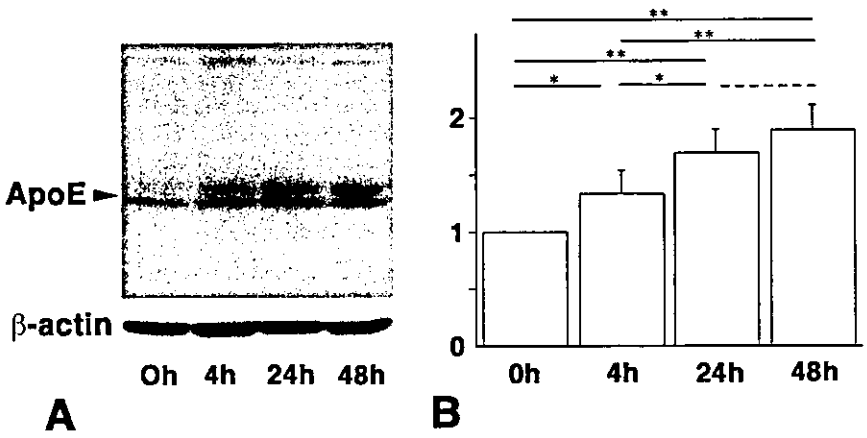

Figure 6. A, Western blot of extracts from human neuroblastoma cell line, GOTO, probed with ApoEC, examined at different intervals after exposure to hydrogen peroxide (0.2 mmol/L). Arrowhead: 36 kDa. β-Actin–immunoreactive bands are shown as an internal control (bottom). B, Quantification of ApoEC-immunoreactive bands expressed as mean of 4 sessions (n=4) at different intervals after challenge with hydrogen peroxide. Relative intensity of ApoEC-immunoreactive bands (mean±SD) was quantified and expressed with intensity at 0 hours (baseline) of each session as a reference, indicated as 1. The increase is statistically significant after 4 hours and thereafter (mean±SD). *$P<0.05$; **$P<0.01$; broken line indicates not significant by ANOVA.

might have visualized ApoE immunoreactivity even in normal neurons,[25] while brain tissue with ischemic focus is usually too fragile to be subjected to such a free-floating method. More importantly, ApoE-like immunoreactivity in neurons was more evident around ischemic foci. Immunoblots from brain extracts demonstrated that full-length form (34 to 37 kDa[2,5,20,26]) of ApoE was present regardless of the disease conditions. Quantification of relative intensity of ApoE-immunoreactive bands demonstrated that the amount of ApoE is increased to 114% (>2-fold) in AD and more significantly increased to 146% in ischemic foci (Figure 5B). Because glial cells in ischemic foci also contain ApoE-like immunoreactivity, it is difficult to decide what kind of cell (neuronal or glial) is responsible for this increase seen on Western blot. Although synthesis of ApoE in other neuroblastoma cell lines has been reported,[4] accumulation of ApoE protein in neuronal cells after exposure to hydrogen peroxide may have some pathological significance.[27] While synthesis of ApoE could be regulated through interaction between glia and neurons, possibly mediated, for example, by nuclear factor-κB,[28,29] the present study on a neuroblastoma cell line demonstrated that neuronal accumulation of ApoE protein could occur independently of glial cells. Therefore, the increase in ApoE, as we observed in ischemic foci of human brains, is explained, at least in part, by upregulation of ApoE synthesis in neurons. Intense ApoE-like immunoreactivity in these neurons in ischemic focus also corroborated this interpretation.

Several epidemiological studies demonstrated that APOE genotype ε4 was possibly linked to some neurological disorders (eg, Lewy body disease, amyotrophic lateral sclerosis, AIDS) other than AD.[30–32] Other studies demonstrated that recovery from cerebrovascular diseases was also influenced by APOE genotype.[33–35] These data suggest that ApoE in the brain plays certain essential roles during destruction and recovery of the nervous system,[33,35] as well as in physiological conditions.[34] It still remains to be proven how ApoE plays certain roles in ischemic foci. The present study suggested an upregulation of ApoE in neurons after cellular stress such as ischemia or oxidative stress. If this upregulation is linked to recovery of neurons after cellular stresses in general, regulation of ApoE expression will provide a clue to constructing a therapeutic strategy aimed at improving recovery from a wide variety of neurological diseases. It is therefore essential to know how the expression of ApoE is regulated in physiological and pathological conditions.

Acknowledgments

This work is supported in part by grants from the Ministry of Culture Science and Education, Japan (128781246), Brain Science Foundation, and Sasagawa Foundation.

References

1. Mahley RW. Apolipoprotein E: cholesterol transport protein with expanding role in cell biology. *Science*. 1988;240:622–630.
2. Ignatius MJ, Gebicke-Härter PJ, Skene JHP, Schilling JW, Weisgraber KH, Mahley RW, Shooter EM. Expression of apolipoprotein E during nerve degeneration and regeneration. *Proc Natl Acad Sci U S A*. 1986; 83:1125–1129.
3. Tomimoto H, Akiguchi I, Suenaga T, Wakita H, Nakamura S, Kimura J, Budka H. Immunohistochemical study of apolipoprotein E in human cerebrovascular white matter lesions. *Acta Neuropathol (Berl)*. 1995;90: 608–614.
4. Dupont-Wallois L, Soulie C, Sergeant N, Wrieze NW, Chartier-Harlin M-C, Delacourte A, Caillet-Boudin M-L. ApoE synthesis in human neuroblastoma cells. *Neurobiol Dis*. 1997;4:356–364.
5. Tesseur I, Dorpe JV, Bruynseels K, Bronfman F, Sciot R, Lommel AV, Leuven FV. Prominent axonopathy and disruption of axonal transport in transgenic mice expressing human apolipoprotein E4 in neurons of brain and spinal cord. *Am J Pathol*. 2000;157:1495–1510.
6. White F, Nicoll JAR, Horsburgh K. Alterations in ApoE and ApoJ in relation to degeneration and regeneration in a mouse model of entorhinal cortex lesion. *Exp Neurol*. 2001;169:307–318.
7. Boyles JK, Pitas RE, Wilson E, Mahley RW, Taylor JM. Apolipoprotein E associated with astrocytic glia of the central nervous system and with nonmyelinating glia of the peripheral nervous system. *J Clin Invest*. 1985;76:1501–1513.
8. Poirier J, Hess M, May PC, Finch CE. Astrocytic apolipoprotein E mRNA and GFAP mRNA in hippocampus after entorhinal cortex lesioning. *Mol Brain Res*. 1991;11:97–106.
9. Namba Y, Tomonaga M, Kawasaki H, Otomo E, Ikeda K. Apolipoprotein E immunoreactivity in cerebral amyloid deposits and neurofibrillary tangles in Alzheimer's disease and kuru plaque amyloid in Creutzfeldt-Jakob disease. *Brain Res*. 1991;541:163–166.
10. Stoll G, Mueller HW, Trapp BD, Griffin JW. Oligodendrocytes but not astrocytes express apolipoprotein E after injury of rat optic nerve. *Glia*. 1989;2:170–176.
11. Han S-H, Hulette C, Saunders AM, Einstein G, Pericak-Vance M, Strittmatter WJ, Roses AD, Schmechel DE. Apolipoprotein E is present in hippocampal neurons without neurofibrillary tangles in Alzheimer's disease and in age-matched controls. *Exp Neurol*. 1994;128:13–26.
12. Han S-H, Einstein G, Weisgraber KH, Strittmatter WJ, Saunders AM, Pericak-Vance M, Roses AD, Schmechel DE. Apolipoprotein E is localized to the cytoplasm of human cortical neurons: a light and electron microscopic study. *J Neuropathol Exp Neurol*. 1994;53:535–544.

13. Uchihara T, Duyckaerts C, He Y, Kobayashi K, Seilhean D, Amouyel P, Hauw J-J. ApoE immunoreactivity and microglial cells in Alzheimer's disease brain. *Neurosci Lett.* 1995;195:5–8.
14. Metzger RE, LaDu MJ, Pan JB, Getz GS, Frail DE, Falduto MT. Neurons of the human frontal cortex display apolipoprotein E immunoreactivity: implications for Alzheimer's disease. *J Neuropathol Exp Neurol.* 1996; 55:372–380.
15. Snipes GJ, McGuire CB, Norden JJ, Freeman JA. Nerve injury stimulates the secretion of apolipoprotein E by nonneuronal cells. *Proc Natl Acad Sci U S A.* 1986;83:1130–1134.
16. Horsburgh K, Nicoll JAR. Selective alterations in the cellular distribution of apolipoprotein E immunoreactivity following transient cerebral ischaemia in the rat. *Neuropathol Appl Neurobiol.* 1996;22:342–349.
17. Horsburgh K, Kelly S, McCulloch J, Higgins GA, Roses AD, Nicoll JAR. Increased neuronal damage in apolipoprotein E-deficient mice following global ischaemia. *Clin Neurosci.* 1999;10:837–841.
18. Dekroon RM, Armati PJ. Synthesis and processing of apolipoprotein E in human brain cultures. *Glia.* 2001;33:298–305.
19. Pitas RE, Boyles JK, Lee SH, Foss D, Mahley RW. Astrocytes synthesize apolipoprotein E and metabolize apolipoprotein E-containing lipoproteins. *Biochim Biophys Acta.* 1987;917:148–161.
20. Schwab C, Steele JC, Akiyama H, McGeer PL. Distinct distribution of apolipoprotein E and β-amyloid immunoreactivity in the hippocampus of Parkinson dementia complex of Guam. *Acta Neuropathol (Berl).* 1996; 92:378–385.
21. Yamakuni T, Usui H, Iwanaga T, Kondo H, Odani S, Takahashi Y. Isolation and immunohistochemical localization of a cerebellar protein. *Neurosci Lett.* 1984;45:235–240.
22. Sekiguchi M, Oota T, Sakakibara K, Inui N, Fujii G. Establishment and characterization of a human neuroblastoma cell line in tissue culture. *Jpn J Exp Med.* 1979;49:67–83.
23. Rebeck GW, Reiter JS, Strickland DK, Hyman BT. Apolipoprotein E in sporadic Alzheimer's disease: allelic variation and receptor interactions. *Neuron.* 1993;11:575–580.
24. Xu P-T, Gilbert JR, Qiu H-L, Ervin J, Rothrock-Christian TR, Hulette C, Schmechel DE. Specific regional transcription of apolipoprotein E in human brain neurons. *Am J Pathol.* 1999;154:601–611.
25. Einstein G, Patel V, Bautista P, Kenna M, Melone L, Fader R, Karson K, Mann S, Saunders AM, Hulette C, et al. Intraneuronal ApoE in human visual cortical areas reflects the staging of Alzheimer disease pathology. *J Neuropathol Exp Neurol.* 1998;57:1190–1201.
26. Huang Y, Liu XQ, Wyss-Coray T, Brecht WJ, Sanan DA, Mahley RW. Apolipoprotein E fragments present in Alzheimer's disease brains induce neurofibrillary tangle-like intracellular inclusions in neurons. *Proc Natl Acad Sci U S A.* 2001;98:8838–8843.
27. Desagher S, Glowinski J, Prémont J. Pyruvate protects neurons against hydrogen peroxide-induced toxicity. *J Neurosci.* 1997;17:9060–9067.
28. Gabriel C, Justicia C, Camins A, Planas AM. Activation of nuclear factor-κB in the rat brain after transient focal ischemia. *Mol Brain Res.* 1999;65:61–69.
29. Petegnief V, Saura J, de Gregorio-Rocasolano N, Paul SM. Neuronal injury-induced expression and release of apolipoprotein E in mixed neuron/glia co-cultures: nuclear factor κB inhibitors reduce basal and lesion-induced secretion of apolipoprotein E. *Neuroscience.* 2001;104:223–234.
30. Saunders AM, Schmader K, Breitner JCS, Benson MD, Brown WT, Goldfarb L, Goldgaber D, Manwaring MG, Szymanski MH, McCown N, et al. Apolipoprotein E ε4 allele distributions in late-onset Alzheimer's disease and in other amyloid-forming diseases. *Lancet.* 1993;342: 710–711.
31. Moulard B, Sefiani A, Laamri A, Malafosse A, Camu W. Apolipoprotein E genotyping in sporadic amyotrophic lateral sclerosis: evidence for a major influence on the clinical presentation and prognosis. *J Neurol Sci.* 1996;139(suppl):34–37.
32. Corder EH, Robertson K, Lannfelt L, Bogdanovic N, Eggertsen G, Wilkins J, Hall C. HIV-infected subjects with the E4 allele for APOE have excess dementia and peripheral neuropathy. *Nat Med.* 1998;4: 1182–1184.
33. Horsburgh K, Graham DI, Stewart J, Nicoll JAR. Influence of apolipoprotein E genotype on neuronal damage and apoE immunoreactivity in human hippocampus following global ischemia. *J Neuropathol Exp Neurol.* 1999;58:227–234.
34. Pedersen WA, Chan SL, Mattson MP. A mechanism for the neuroprotective effect of apolipoprotein E: isoform-specific modification by the lipid peroxidation product 4-hydroxynonenal. *J Neurochem.* 2000;74: 1426–1433.
35. Horsburgh K, McCulloch J, Nilsen M, Roses AD, Nicoll JAR. Increased neuronal damage and apoE immunoreactivity in human apolipoprotein E, E4 isoform-specific, transgenic mice after global cerebral ischaemia. *Eur J Neurosci.* 2000;12:4309–4317.

Neuropathology 2003; **23**, 318–326

Symposium: Neuropathological Criteria for Neurodegenerative Diseases

Pick body disease and Pick syndrome*

Toshiki Uchihara,[1] Kenji Ikeda[2] and Kuniaki Tsuchiya[3]

[1]Department of Neuropathology, Tokyo Metropolitan Institute for Neuroscience, [2]Department of Psychogeriatrics, Tokyo Institute of Psychiatry and [3]Department of Laboratory Medicine and Pathology, Tokyo Metropolitan Matsuzawa Hospital, Tokyo, Japan

Diagnostic criteria for Pick's disease have been criticized from many different viewpoints. This confusion is mainly derived from the ambiguity of this term 'Pick's disease' (PD), which may imply either purely histological findings, such as Pick body (PB), or a characteristic clinical syndrome that could occur even in the absence of PB. This taxonomic confusion will be circumvented by introducing the diagnostic term 'Pick body disease' to designate patients with the characteristic argyrophilic inclusions purely on histological grounds. In parallel, employment of 'Pick syndrome' to describe the time-honored clinical features may be more convenient and less confusing than PD because PD implies either the presence of PB or the clinical features, two aspects not necessarily linked to each other. Three-dimensional reconstruction of PB confirmed that tau-like immunoreactivity was accentuated at their periphery, as was recognized with the Bodian method. Preferential affinity of three-repeat tau pathology, as seen in Pick body disease, to the Bodian over the Gallyas method is distinct from the reversed affinity (the Gallyas over the Bodian method) of four-repeat tau pathology, as seen in corticobasal degeneration and in argyrophilic grains. This preference of silver staining is compatible with the mixed three- and four-repeat tau pathology, as seen in NFT of the Alzheimer's type, which are stained with both the Bodian and Gallyas staining. This will provide a practical basis on which to differentiate these disorders based on their distinctive tau species and possible relation of tau species to staining profile on these silver methods.

Key words: 3-D reconstruction, diagnostic criteria, Pick body, silver staining, three-repeat tau.

Correspondence: Toshiki Uchihara, Department of Neuropathology, Tokyo Metropolitan Institute for Neuroscience, 2-6 Musashi-dai, Fuchu, Tokyo 183-8526, Japan. Email:uchihara@tmin.ac.jp

*Presented at the 44th Annual Meeting of the Japanese Society of Neuropathology, Nagoya, 30 May 2003.

Received 30 June 2003; accepted 7 July 2003.

INTRODUCTION

Diagnostic criteria for Pick's disease (PD) have been a matter of considerable debate primarily because the definition of the disease is highly variable and dependent on viewpoint.[1–3] So far, none of the diagnostic criteria for PD have been satisfactory, having never been free from some ambiguity and criticism.[4,5] In the present paper we tried to delineate potential controversies related to the nosology of PD by tracing the historical background to its original description.[6] We then became aware that the ambiguity of PD could be circumvented if this term is dissected to emphasize the different viewpoints: 'Pick body disease',[7] which is concerned with purely histological features, and 'Pick syndrome' to describe exclusively clinical characteristics with macroscopic atrophy of the cerebral cortex now detectable even in life with imaging techniques.[8] These two different aspects are often observed in a single patient but have no semantic relation to each other, therefore, could be applied independently. This reduction in ambiguity after employing this parallel terminology will simplify the debate concerning the nosology of PD. Although this is proposed in order to escape the taxonomic confusion, it will be useful and convenient for clinicopathological understanding and communications on this disease, which will provide a unified framework shared among those interested in this disease.

HOW TO IDENTIFY AND DEFINE NEUROLOGICAL DISEASES IN THE AGING BRAIN

A diagnostic guideline for a certain disease is usually based on its original description. Clinical criteria are sometimes useful but they do not always provide a firm basis on which to delineate the disease and one may usually ask for pathological alterations that corroborate the specificity of the disease in order to define it more precisely. One of the difficulties in defining PD is that its original description dealt

Table 1 Guide to establishment of diagnostic criteria

Basis for definition	Extent/quantity of the lesion	Concept of disease entity
Examples	Alzheimer's disease	Pick's disease
	Lewy body disease	ALS-D
	Tangle-only dementia	CBD/PSP
Nature of definition	Operational	Conceptual
Measure for definition	Quantitative	Qualitative
Age-related change	Linked	Not linked
Threshold	Through statistics	No threshold
Diagnostic inference	Probabilistic	All or non
Exceptional cases	Inherently present	May change the concept
Criteria	Resistant to falsification	Fragile, if falsified

ALS-D, amyotrophic lateral sclerosis with dementia; CBD, corticobasal degeneration.

mainly with aphasic symptoms and its possible link to a circumscribed atrophy of the cerebral cortex without providing microscopic data.[9] This left a considerable ambiguity, which, in turn, allowed a wide variety of interpretations by subsequent researchers with different viewpoints.[10]

Neuropathological examination of the brain is sometimes hampered by concomitant lesions such as senile plaques (SP), NFT and Lewy bodies, each believed to be linked to the aging process.[11-14] Sound interpretation therefore, should take these lesions into consideration so that pathological processes out of these aging-associated changes can be isolated. As shown in Table 1, several diseases are characterized by these aging-associated changes by themselves. Therefore, criteria for these diseases are obliged to deal with the quantity of the lesions in question. One of the practical and prevailing approaches is a statistical analysis of these quantitative data to define a threshold.[15-20] This is, however, just an operational threshold that is tentatively agreed to discriminate a disease-equivalent quantity from the normal range but represents neither the cause nor entire process of the disease. When this statistics-based evidence is applied to the diagnosis, one should be aware that this probabilistic attitude inherently is not free from a diagnostic error, defined as sensitivity and specificity. For example, the abundance of SP that fulfills the criteria for AD could be found in a small fraction of individuals without dementia.[14,21] A similar discrepancy can be found with NFT or Lewy bodies.[19,20,22] Moreover, application of the same protocol does not always reach the same diagnosis because the definition of a threshold is greatly influenced by the procedures that visualize lesions in question, but differently organized in each laboratory. What is worse, different experts, even when dealing with the same histological section, may report conflicting interpretations.[23,24]

On the contrary, several abnormal pathological structures are never encountered during normal physiological aging. Examples of this are PB in PD,[25] Bunina bodies in amyotrophic lateral sclerosis (ALS) and ubiquitin-positive inclusions in ALS with dementia (ALS-D).[26-29] One of the diagnostic hallmarks for AD is NFT. Their appearance in the motor cortex, basal ganglia and in pontine nuclei, however, is not usual in AD or in aging brains, thus they could be a hallmark for PSP.[30] They are then reliably incorporated into the diagnostic criteria if they are the principal hallmark for the disease. Here, again, we are still confronted with a difficulty in defining PD because it remains to be determined whether PD can be defined based merely on the presence of PB.[31]

PICK-TYPE ATROPHY OR PB, AS A MORPHOLOGICAL SUBSTRATE FOR PD?

Onari and Spatz proposed their definition of PD in 1926.[31] Following is a summary of their criteria.

1 Macroscopic atrophy in the temporal or frontal lobe.
2 Characteristic preservation of the first temporal gyrus, transverse gyrus and Ammon's horn.
3 Primary degenerative changes in the cortical gray matter, with concomitant involvement in the corresponding white matter.
4 Neuronal depletion accentuated in the superficial cortical layers I-IIIa.
5 Occasional presence of ballooned neurons.
6 Absence of atherosclerosis, inflammatory changes, NFT and SP.
7 Occasional presence of PB (*Die argentophilen Kugeln Alzheimers*), that are not influential on the entire clinicopathological features.

Their criteria relied heavily on macroscopic findings, which presumably correspond to clinical manifestations, while the presence of PB or ballooned neurons were considered to be not influential on this atrophy and clinical picture. In the former half of the 20th century, even gross morphological changes were not detectable before autopsy. It is important to reconsider that it is only recently that clinicians have access to macroscopic findings of the brain before autopsy. Neuropathologists in those days

therefore payed equivalent attention to both macroscopic and microscopic findings, and trained neuropathologists could sometimes be so confident of their macroscopic diagnosis that microscopic examination was not always considered necessary, as declared in an anecdote 'Low-power pathologists have a high power' (MP Valsamis, pers. comm., 1995) It was therefore reasonable that Onari and Spatz considered the characteristic clinical picture and corresponding cortical atrophy as a combined hallmark for PD, rather than inconsistent and less influential microscopic lesions, probably expecting that PD could be placed in recognizable contrast to AD.[32] Indeed, this concept gradually gained acceptance and has been useful for clinical diagnosis and corresponding pathological verification as PD. After introduction of brain imaging, however, it is the clinician who is the first to be aware of the distribution of atrophy in the living patients.[33] Nowadays neuropathologists are not only informed of the distribution and extent of brain atrophy but also even of functional status of the brain before the autopsy. This innovation in imaging during clinical diagnosis allowed clinicians to gain access to the macroscopic findings of the diseased brain prior to neuropathologists. Needless to say, it is still essential for the neuropathologists to pay attention to macroscopic findings of the brain. However, macroscopic observation are now open to clinicians and some say that *in vivo* observation through brain imaging may even be closer to the reality than the post-mortem examination. Microscopic observation is now the sole remaining field wherein neuropathologists are the exclusive interpreters. This presumably prompted neuropathologists to concentrate on microscopic findings in more detail.

Pick body disease with or without dementia

Although it has been reported as if cases with PB were always associated with typical cortical atrophy as described by Onari and Spatz, subsequent studies, however, identified several patients with PB having a distribution of cortical lesions that was different from those described by Onari and Spatz. For example, a circumscribed atrophy of the parietal cortex has been described by different authors.[34–36] A degenerative process with PB accentuated in the convexity of the frontal lobe was described in a patient diagnosed as having depressive state without dementia.[37] These examples indicate that the presence of PB is not restricted to patients with typical clinical presentation of dementia but is extended to other cases with cortical dysfunction not necessarily related to dementia. If we labeled these patients without dementia with the diagnosis of PD it would be very confusing because PD has been considered to represent a kind of dementing disease different from AD. One of the ways to circumvent this confusion is to use the diagnostic term 'Pick body disease', which is linked directly to the mere presence of PB regardless of the clinical presentation.[7] In most cases the presence of PB correlated with typical clinical presentation with dementia but is to be extended rarely to other clinical manifestations not necessarily related to dementia. Once the designation of 'Pick body disease' is employed, this terminology is not only convenient to avoid unnecessary confusion regarding the non-demented cases with PB but also suggests a pathological cascade shared among cases characterized by the presence of PB.

Pick syndrome as a time-honored clinicopathological entitiy

Is it then reasonable to abandon the name of PD because of its ambiguity after employment of Pick body disease?[38–40] The authors' understanding is that PD is a clinicopathological entity, as defined by Onari and Spatz, with special reference to clinical picture of dementia and the corresponding atrophy in the cerebral cortex, irrespective of the presence of PB.[31] Clinical diagnosis of PD therefore may be useful and acceptable for patients with characteristic dementia and cortical atrophy typical for PD as initially delineated by Onari and Spatz.[31] Furthermore, it will well characterize the clinical picture better than the more loosely defined term 'frontotemporal dementia' (FTD) because the latter potentially includes a wide variety of dementias, with that of highest severity named 'Pick-type FTD', to very mildly demented patients mostly recognized as ALS-D.[41] We agree that FTD is a convenient diagnostic flag that includes a wide range of non-Alzheimer-type dementias. This convenience may, however, potentially obscure the clinical features of time-honored characteristics of PD, in return.[42,43] But even if these cases are called PD, another ambiguity arises as to whether this diagnosis implies the presence of PB in addition to the clinical picture or whether it describes characteristic dementia with corresponding atrophy irrespective of the presence of PB. One of the ways to avoid this confusion will be to use the term 'Pick syndrome', which has no semantic relevance to PB. It is now known that other defined entities, such as corticobasal degeneration (CBD),[44] dementia with argyrophilic grains[45] and ALS-D,[46] possibly exhibit severe cortical involvement, clinically indistinguishable from PD. Pick syndrome will potentially include these situations irrespective of the microscopic findings. Arnold Pick, one of the greatest neurologist–psychiatrists to date,[47] will supposedly be much more satisfied if this characteristic dementing condition is still being crowned with his name rather than having his name confined to tiny intraneuronal inclusions. Authors will be happy if he agrees to our proposal to use his name for 'Pick body disease', as well as 'Pick syndrome'.

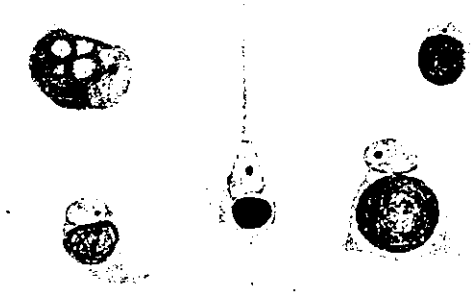

Eigentümliche Fibrillenveränderung der Ganglienzellen in einem Fall von umschriebener seniler Atrophie. Bielschowsky-Präparat.

Fig. 1 Argentophilic inclusions (PB) initially described by Alois Alzheimer (Bielschowsky preparation).[25]

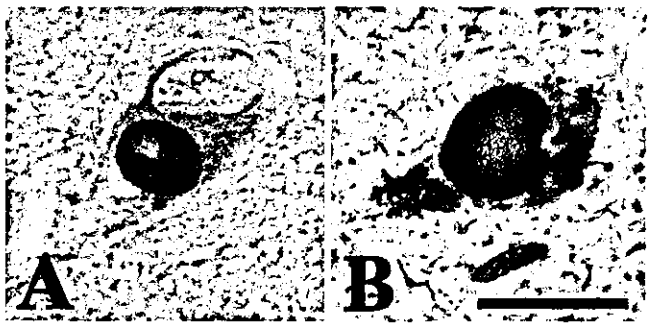

Fig. 2 Silver-staining of PB in the pyramidal neurons of hippocampus. (A) Bielshowsky staining; (B) Bodian staining. (Bar = 20 μm).

PICK BODIES

Argyrophilia and 3-D structure of Pick bodies

In order to employ the PB as a diagnostic flag, it is necessary to clarify the nature of PB in order to be readily applicable for morphological diagnosis. It was Alois Alzheimer who first identified argyrophilic inclusions in the neurons in a brain with circumscribed atrophy.[25] He labeled this inclusion *Fibrillenveränderung* (Fig. 1) but it was later proved to be different from NFT seen in AD brains and is currently called PB. This original description by Alzheimer was based on sections stained with the Bielschowsky method (Fig. 2A). Pick bodies are usually round with an occasional indentation in the aspect facing the nucleus.[48] The argyrophilic property of PB is sometimes intensified at the periphery, which is readily detectable on Bodian-stained sections (Fig. 2B). Argyrophilia inside the PB is usually homogeneous but sometimes exhibits discontinuity or unstained regions, as initially noted by Alzheimer (Fig. 1 upper left; Fig. 2A).[25]

Pick bodies are intensely labeled with anti-tau antibodies but ubiquitin-like immunoreactivity is inconsistent.[49–52]

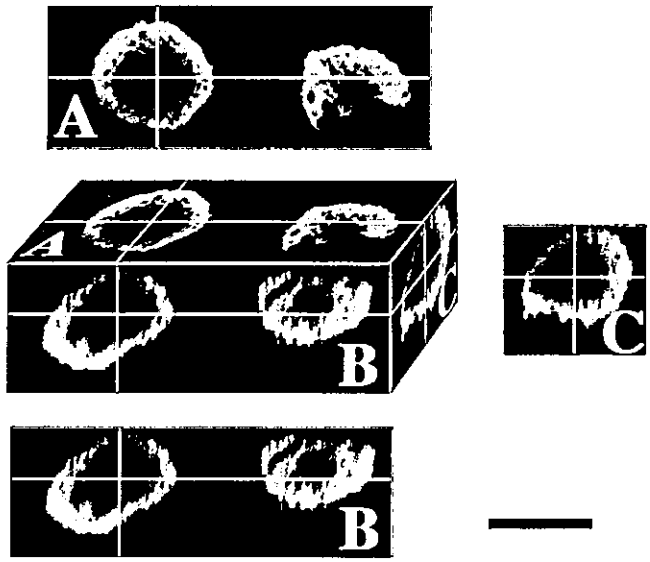

Fig. 3 Immunostaining with anti-paired-helical filaments tau (AT8) visualized with fluorescein-isothiocyanate and their 3-D reconstruction. (A) Original upper view. Serial optical section parallel to (A) were obtained at an interval of 0.1 μm to include the entire structure of PB. These images were reconstructed using software (3D-volume, Ratoc, Tokyo, Japan) to be observed as front view (B) or side view (C), at any arbitrary plane, indicated with white lines. (Bar = 10 μm).

Immunofluorolabeling with an anti-paired-helical filaments tau antibody (AT8) clarified that there are some PB with their tau-like immunoreactivity intensified at their periphery, leaving their central portion less stained (Fig. 3). Serial optical sections at an interval of 0.1 μm were obtained with a confocal microscope (TCS/SP, Leica, Heidelberg, Germany) from the immunofluolabeled sections, so that the entire structure of the PB is to be reconstructed on a 3-D basis on specialized software (3D-Volume, Ratoc, Tokyo, Japan) run on a Windows platform. As was seen with the Bodian method (Fig. 2B), tau-like immunoreactivity in the PB was intensified at the periphery, leaving the central portion less stained. This is compatible with the electron-microscopical observation on PB that the fibers are sometimes more crowded at the periphery of the PB.[53]

Silver staining methods and their possible relation to tau-isoforms

We should, however, pay attention to argyrophilia of the PB, which is highly dependent on the staining procedure employed. The Bodian method and Bielschowsky method are appropriate to stain PB. Figure 4 demonstrates double-stained fluorescence with AT8-FITC (Fig. 4B) and thiazin red (Fig. 4A), a fluorochrome that has an affinity to fibrillary structures such as NFT or Lewy bodies. After the double-fluorescence image was recorded, the section was

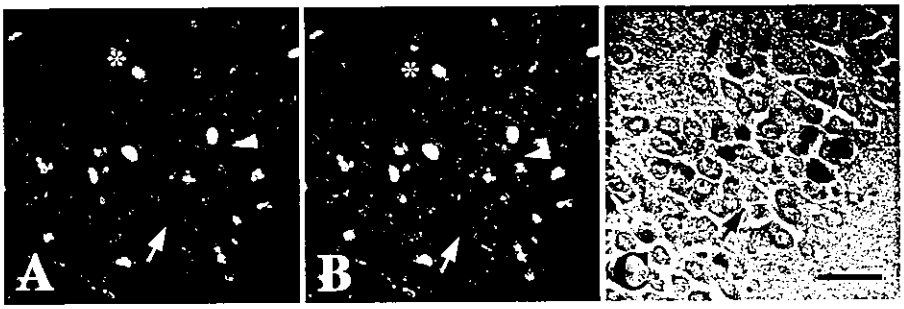

Fig. 4 Hippocampal dentate gyrus of Pick body disease. (A) Thiazin red (TR), a fluorochrome with affinity to fibrillary structure; (B) Anti-paired-helical filaments tau (AT8) immunoreactivity; (C) the same microscopic field as (A,B) on the same section stained with the Gallyas method. The affinity of PB to TR and the Gallyas method is highly variable. AT8 immunoreactivity accompanied by TR and Gallyas (*) is exceptional. Some are positive only for AT8 (arrow) or accompanied by Gallyas method (arrowhead). Bar = 50 μm.

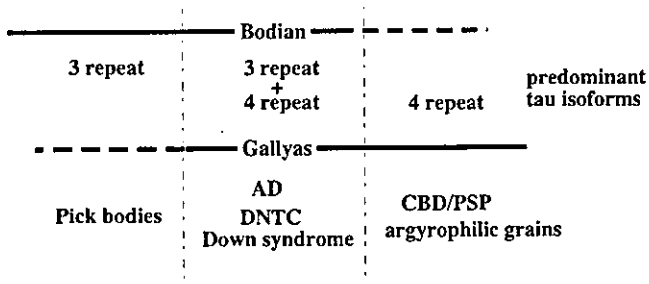

Fig. 5 Tau-positive structures in neuron and their argentophilic property with possible relation to tau isoforms. The PB are predominantly of three-repeat tau pathology, preferentially stained with Bodian over Gallyas method. Neuronal tau-positive structures in corticobasal degeneration (CBD) and argyrophilic grains are of four-repeat tau pathology, preferentially stained with Gallyas over Bodian method. The NFT in AD, diffuse NFT with calcification (DNTC) and Down syndrome are of mixed three- and four-repeat tau pathology, stained with both the Gallyas and the Bodian method.

subjected to the Gallyas method and the same structures were identified (Fig. 4C) to examine the relationship between fluorescent signals and the argyrophilia. This procedure demonstrated that AT8-positive PB were rarely stained with the Gallyas method.[54] Table 2 shows the quantitative data that demonstrate the difference in the staining profiles in so-called degenerative tauopathies. It is apparent that most of the PB are characterized by the paucity of argyrophilia with the Gallyas method (38.3% + 28.2% = 66.5%; Table 2, □) while other tau-positive structures including pretangle neurons, NFT of AD and of diffuse NFT with calcification, and tau-positive neurons in the CBD are intensely stained with the Gallyas method (Table 2, ⬚). On the contrary, the Bodian method stains PB and NFT while tau-positive neurons in CBD are rarely stained with the Bodian method.[55] Figure 5 demonstrates the overall relation between tau-positive structures and their argyrophilia. The Bodian method stains PB but not tau-positive structures in CBD. In contrast, the Gallyas method stains tau-positive structures in CBD, and argyrophilic grains, both of which are less intensely stained with the Bodian method. The NFT are stained with both the Gallyas method and the Bodian method. It has been erroneously considered that the Gallyas method is far more sensitive than the Bodian method in detecting tau-positive structures irrespective of the lesions. Our observation, however, indicates that the difference of these two silver staining methods is based on the different nature of the lesions[56,57] rather than difference in the sensitivity. One of the recent advances in classifying these degenerative tauopathies is based on the biochemical nature of tau according to its molecular species, three-repeat or four-repeat tau. If a major tau abnormality in PB disease is predominantly related to its three-repeat isoform,[58] then the preferential affinity of PB to the Bodian method with scarce affinity to the Gallyas method (Bod+/Gal–) may correspond to this biochemical abnormality. It is interesting that tau-positive structures in CBD[59] and argyrophilic grain disease[60] both related to an abnormality in four-repeat tau, are conversely stained preferentially with the Gallyas method (Bod–/Gal+). This possible correlation between tau isoforms and argyrophilic profiles (Bod+/Gal– for three-repeat and Bod–/Gal+ for four-repeat tau pathology) is still compatible with NFT, with mixed three- and four-repeat abnormality, because they are stained with both the Bodian and Gallyas method (Bod+/Gal+).[59] Up to now, almost all antibodies against tau immunolabel these structures. Although distinction of these tauopathies with tau-immunohistochemistry is a challenge for neuropathologists, no immunohistochemical approaches available to date have been very successful in discriminating these differences. In contrast, it is possible to classify these tau-immunoreactive structures further with silver staining methods in a disease-specific fashion. We know little of how these silver staining procedures display argyrophilia[56,57] to some characteristic pathological structures relevant to specific pathological conditions. This lack of molecular explanation is one of the major criticisms from modern neuroscientists, convinced that procedures,

Table 2 Tau-like immunoreactivity and its relation to argyrophilia by Gallyas method

Gallyas	−	−	+	+	+	+	−	Per 10 fields
AT8	+	+	+	+	−	−	−	
Th. Red	−	+	−	+	+	−	+	
PBD ($n = 4$)	42.0	31.0	1.9	26.6	0.3	7.6	0.4	109.8
(%)	(38.3)	(28.2)	(1.8)	(24.2)	(0.2)	(6.9)	(0.4)	
CBD ($n = 6$)	0.1	0	11.4	2	0	2.6	0	16.1
(%)	(0.5)	(0)	(70.8)	(12.3)	(0)	(16.4)	(0)	
AD ($n = 5$)	0.2	0	1.7	46.1	23.2	0.9	2.1	74.3
(%)	(0.3)	(0)	(2.3)	(62.0)	(31.3)	(1.2)	(2.8)	
DNTC ($n = 3$)	0	0.3	0.1	21.7	71.8	24.7	0.3	118.9
(%)	(0)	(0.2)	(0.1)	(18.2)	(60.4)	(20.8)	(0.2)	

Staining profiles of each structure classified according to Gallyas method, anti-paired-helical filament tau anitbody (AT8) immunoreactivity, and fluorescence from thiazin red (Th. Red). Most of the PB are (□) AT8+/Gallya−, while other AT8-positive structures are (⬚) also positive for Gallyas (AT8+/Gallyas+). PBD, Pick body disease; CBD, corticobasal degeneration; DNTC, diffuse neurofibrillary tangles with calcification.
Modified from Uchihara *et al.*[54]

such as silver staining, are not reliable. It is, however, obvious that additional procedures will give additional information from different viewpoints as we demonstrated with different silver staining methods on tau-positive structures. This kind of information, even without molecular explanation, could be sometimes useful in identifying lesions and their pathological differentiation. Moreover, the immunohistochemical approach could be as unstable as silver staining and its biased attention to a single epitope will make the examiners blinded to factors other than the epitope under current interest. Sound interpretation will therefore be maximized when several techniques, classical stainings, silver stainings and immunohistochemical procedures are combined.

CONCLUSIONS

Diagnostic criteria for PD have been confronted with criticisms from different viewpoints. This confusion is derived from an ambiguity of this term that may potentially imply either purely histological findings, such as PB, or a clinical syndrome that could occur even in the absence of PB. We then propose the diagnostic term 'Pick body disease' to designate cases with characteristic argyrophilic inclusions purely on histological grounds. In parallel, it will be convenient to use 'Pick syndrome' to describe the time-honored clinical features because PD may possibly imply the presence of PB rather than the clinical features. This parallel terminology will be convenient in avoiding taxonomic confusion around PD. Recent biochemical analysis clarified that Pick body disease is linked to a modification of three-repeat tau protein. A possible association of this biochemical abnormality to preferential staining with the Bodian method is in contrast with preferential staining with the Gallyas method on four-repeat tau abnormality in CBD or in argyrophilic grain disease. This discrimination may reflect some distinctive pathological processes and could be useful, at present, for diagnostic differentiation. Immunohistochemical examination combined with silver-stained features in relation to biochemical findings will give a comprehensive understanding of the disease process. This will be not only helpful in making the diagnostic criteria more precise but also in understanding characteristic aspects of the disease processes.

ACKNOWLEDGMENTS

Authors are grateful to Ms Ayako Nakamura, Department of Neuropathology, Tokyo Metropolitan Institute for Neuroscience, for her excellent histological preparations. Authors are also grateful to professor Kenji Kosaka, Department of Psychiatry, Yokohama City University, Yokohama, Japan, Professor Jean-Jacques Hauw, Professor Charles Duyckaerts, Laboratoire Raymond Escourolle, Hôpital de la Salpêtrière, Paris, France and Dr Kunimasa Arima, Department of Laboratory Medicine, National Center Hospital for Mental, Nervous, and Muscular Disorders, National Center for Neurology and Psychiatry, Tokyo, Japan, for fruitful discussions. This work is supported in part by the grants (TU) from the Ministry of Health and Welfare (Longevity Science H-14–005) and from the Ministry of Education, Culture, Sports, Science and Technology (grant-in-aid for scientific research B15300118).

REFERENCES

1. Rossor MN. Pick's disease: a clinical overview. *Neurology* 2001; **56**: S3–S5.
2. Tsuchiya K. History and transition of concept in Pick disease (in Japanese). *Shinkei-Naika [Neurol Med]* 1999; **50**: 321–328.

3. Constantinidis J, Richard J, Tissot R. Pick's disease. Histological and clinical correlations. *Eur Neurol* 1974; **11**: 208–217.
4. Duyckaerts C, Dürr A, Uchihara T, Boller F, Hauw J-J. Pick complex: too simple? *Eur J Neurol* 1996; **3**: 283–286.
5. Duyckaerts C, Hauw JJ. Diagnostic controversies: another view. *Adv Neurol* 2000; **82**: 233–240.
6. Karenberg A. Zur Frühgeschichte der Pickschen Erkrankung. *Fortschr Neurol Psychiatry* 2001; **69**: 545–550.
7. Uchihara T, Tsuchiya K. Pick body disease: a proposal. *Neuropathology* 2000; **20**: 246.
8. Uchihara T. Neuropathology of Pick syndrome (in Japanese). *Shinkei-Naika [Neurol Med]* 1999; **50**: 342–348.
9. Pick A. Ueber die Beziehungen der senilen Hirnatrophie zur Aphasie. *Prager Med Wochenschr* 1892; **17**: 165–167.
10. Escourolle R. La maladie de Pick (Étude critique d'ensemble et synthèse anatomoclinique). Thesis, Université de Paris, Paris, France, 1956.
11. Inose T. Die Histopathologie des Senilen Gehirns (in Japanese). *Seishin Shinkeigaku Zasshi* 1955; **57**: 63–96.
12. Tomlinson BE, Blessed G, Roth M. Observations on the brains of non-demented old people. *J Neurol Sci* 1968; **7**: 331–356.
13. Matsushita M. Neuropatholgy of physiological ageing brain (in Japanese). *Shinkei Shinpo [Adv Neurol]* 1985; **29**: 564–575.
14. Katzman R, Terry RD, DeTeresa R. Clinical, pathological, and neurochemical changes in dementia: a subgroup with preserved mental status and numerous neocortical plaques. *Ann Neurol* 1988; **23**: 138–144.
15. Mirra SS, Heyman A, McKeel D *et al.* The Consortium to Establish a Registry for Alzheimer's Disease (CERAD). Part II. Standardization of the neuropathologic assessment of Alzheimer's disease. *Neurology* 1991; **41**: 479–486.
16. Gearing M, Mirra SS, Hedreen JC, Sumi SM, Hansen LA, Heyman A. The Consortium to Establish a Registry for Alzheimer's Disease (CERAD). Part X. Neuropathology confirmation of the clinical diagnosis of Alzheimer's disease. *Neurology* 1995; **45**: 461–466.
17. Newell KL, Hyman BT, Growdon JH, Hedley-Whyte ET. Application of the National Institute on Aging (NIA)–Reagan Institute criteria for the neuropathological diagnosis of Alzheimer disease. *J Neuropathol Exp Neurol* 1999; **58**: 1147–1155.
18. Halliday G, Ng T, Rodriguez M *et al.* Consensus neuropathological diagnosis of common dementia syndromes: testing and standardising the use of multiple diagnostic criteria. *Acta Neuropathol (Berl)* 2002; **104**: 72–78.
19. McKeith IG, Perry EK, Perry RH. Report of the second dementia with Lewy body international workshop: diagnosis and treatment. Consortium on Dementia with Lewy Bodies. *Neurology* 1999; **53**: 902–905.
20. McKeith IG, Ballard CG, Perry RH *et al.* Prospective validation of consensus criteria for the diagnosis of dementia with Lewy bodies. *Neurology* 2000; **54**: 1050–1058.
21. Delaère P, Duyckaerts C, Masters C, Piette F, Hauw JJ. Large amounts of neocortical βA4 deposits without Alzheimer changes in a nondemented case. *Neurosci Lett* 1990; **116**: 87–93.
22. Forno LS. Concentric hyalin intraneuronal inclusions of Lewy type in the brains of elderly persons (50 incidental cases): relationship to parkinsonism. *J Am Geriatr Soc* 1969; **17**: 557–575.
23. Duyckaerts C, Delaère P, Hauw JJ *et al.* Rating of the lesions in senile dementia of the Alzheimer type: concordance between laboratories. A European multicenter study under the auspices of EURAGE. *J Neurol Sci* 1990; **97**: 295–323.
24. Mirra SS, Gearing M, McKeel Jr DW *et al.* Interlaboratory comparison of neuropathology assessments in Alzheimer's disease: a study of the Consortium to Establish a Registry for Alzheimer's Disease (CERAD). *J Neuropathol Exp Neurol* 1994; **53**: 303–315.
25. Alzheimer A. Über eigenartige Krankheitsfälle des späteren Alters. *Z Ges Neurol Psychiatrie* 1911; **4**: 356–385.
26. Okamoto K, Hirai S, Yamazaki T, Sun X, Nakazato Y. New ubiquitin-positive intraneuronal inclusions in the extramotor cortices in patients with amyotrophic lateral sclerosis. *Neurosci Lett* 1991; **129**: 233–236.
27. Mitsuyama Y. Presenile dementia with motor neuron disease in Japan: clinico-pathological review of 26 cases. *J Neurol Neurosurg Psychiatry* 1984; **47**: 953–959.
28. Yuasa R. Amyotrophic lateral sclerosis with dementia (in Japanese). *Clin Neurol* 1970; **10**: 569–577.
29. Yoshida M, Murakami N, Hashizume Y, Takahashi A. A clinicopathological study on 13 cases of motor neuron disease with dementia (in Japanese). *Clin Neurol* 1992; **32**: 1193–1202.
30. Hauw JJ, Verny M, Delaère P, Cervera P, He Y, Duyckaerts C. Constant neurofibrillary changes in the neocortex in progressive supranuclear palsy. Basic differences with Alzheimer's disease and aging. *Neurosci Lett* 1990; **119**: 182–186.

31. Onari K, Spatz H. Anatomische Beiträge zur Lehre von der Pickschen umschriebene Großhirnrinden-Atrophie ('Picksche Krankheit'). *Z Ges Neurol Psychiatrie* 1926; **101**: 470–511.
32. Delay J, Brion S, Badaracco JG. Le diagnostic différentiel des maladie de Pick et d'Alzheimer. à propos de 12 observations anatomo-cliniques. *Encéphale* 1955; **44**: 454–499.
33. Fukui T, Kertesz A. Volumetric study of lobar atrophy in Pick complex and Alzheimer's disease. *J Neurol Sci* 2000; **174**: 111–121.
34. Lang AE, Bergeron C, Pollanen MS, Ashby P. Parietal Pick's disease mimicking cortical-basal ganglionic degeneration. *Neurology* 1994; **44**: 1436–1440.
35. Fukui T, Sugita K, Kawamura M, Shiota J, Nakano I. Primary progressive apraxia in Pick's disease: a clinicopathologic study. *Neurology* 1996; **47**: 467–473.
36. Cambier J, Masson M, Dairou R, Henin D. Étude anatomo-clinique d'une forme pariétale de maladie de Pick. *Rev Neurol (Paris)* 1981; **137**: 33–38.
37. Tsuchiya K, Ikeda M, Hasegawa K *et al.* Distribution of cerebral cortical lesions in Pick's disease with Pick bodies: a clinicopathological study of six autopsy cases showing unusual clinical presentations. *Acta Neuropathol (Berl)* 2001; **102**: 553–571.
38. Baldwin B, Forstl H. 'Pick's disease': 101 years on still there, but in need of reform. *Br J Psychiatry* 1993; **163**: 100–104.
39. Kertesz A. What are the obstacles for an accurate clinical diagnosis of Pick's disease? *Neurology* 1998; **50**: 1192–1193.
40. Litvan I, Agid Y, Sastry N *et al.* What are the obstacles for an accurate clinical diagnosis of Pick's disease? A clinicopathologic study. *Neurology* 1997; **49**: 62–69.
41. Ikeda K, Akiyama H, Arai T, Ueno H, Tsuchiya K, Kosaka K. Morphometrical reappraisal of motor neuron system of Pick's disease and amyotrophic lateral sclerosis with dementia. *Acta Neuropathol (Berl)* 2002; **104**: 21–28.
42. Hodges JR. Frontotemporal dementia (Pick's disease): clinical features and assessment. *Neurology* 2001; **56**: S6–S10.
43. Ikeda K. Clinical feature of Pick disease. Viewpoint from a psychiatrist (in Japanese). *Shinkei-Naika [Neurol Med]* 1999; **50**: 335–341.
44. Miyazaki H, Saito Y, Kijima Y, Akabane H, Tsuchiya K. An autopsy case of corticobasal degeneration mimicking frontal Pick's disease (in Japanese). *No Shinkei* 1997; **49**: 277–282.
45. Tsuchiya K, Mitani K, Arai T *et al.* Argyrophilic grain disease mimicking temporal Pick's disease: a clinical, radiological, and pathological study of an autopsy case with a clinical course of 15 years. *Acta Neuropathol (Berl)* 2001; **102**: 195–199.
46. Tsuchiya K, Ikeda K, Haga C *et al.* Atypical amyotrophic lateral sclerosis with dementia mimicking frontal Pick's disease: a report of an autopsy case with a clinical course of 15 years. *Acta Neuropathol (Berl)* 2001; **101**: 625–630.
47. Kertesz A, Kalvach P. Arnold Pick and German neuropsychiatry in Prague. *Arch Neurol* 1996; **53**: 935–938.
48. Arima K. Pathological features of Pick bodies (in Japanese). *Shinkei-Naika [Neurol Med]* 1999; **50**: 349–356.
49. Probst A, Anderton BH, Ulrich J, Kohler R, Kahn J, Heitz PU. Pick's disease: an immunocytochemical study of neuronal changes. Monoclonal antibodies show that Pick bodies share antigenic determinants with neurofibrillary tangles and neurofilaments. *Acta Neuropathol (Berl)* 1983; **60**: 175–182.
50. Rasool CG, Selkoe DJ. Sharing of specific antigens by degenerating neurons in Pick's disease and Alzheimer's disease. *N Engl J Med* 1985; **312**: 700–705.
51. Love S, Saitoh T, Quijada S, Cole GM, Terry RD. Alz-50, ubiquitin and tau immunoreactivity of neurofibrillary tangles, Pick bodies and Lewy bodies. *J Neuropathol Exp Neurol* 1988; **47**: 393–405.
52. Murayama S, Mori H, Ihara Y, Tomonaga M. Immunocytochemical and ultrastructural studies of Pick's disease. *Ann Neurol* 1990; **27**: 394–405.
53. Oyanagi S. Ultrastructural comparison between Pick bodies and the neurofibrillary changes in Alzheimer's disease and progressive supranuclear palsy. In: Hirano A, Miyoshi K (eds) *Neuropsychiatric Disorders in the Elderly.* Tokyo: Igaku Shoin, 1983; 118–126.
54. Uchihara T, Nakamura A, Yamazaki M, Mori O, Ikeda K, Tsuchiya K. Different conformation of neuronal tau deposits distinguished by double immunofluorescence with AT8 and thiazin red combined with Gallyas method. *Acta Neuropathol* 2001; **102**: 462–466.
55. Uchihara T, Mizusawa H, Tsuchiya K, Kondo H, Oda T, Ikeda K. Discrepancy between tau immunoreactivity and argyrophilia by the Bodian method in neocortical neurons of corticobasal degeneration. *Acta Neuropathol* 1998; **96**: 553–557.
56. Iqbal K, Braak E, Braak H, Zaidi T, Grundke-Iqbal I. A silver impregnation method for labeling both Alzheimer paired helical filaments and their polypeptides separated by sodium dodecyl sulfate-polyacrylamide gel electrophoresis. *Neurobiol Aging* 1991; **12**: 357–361.
57. Gambetti P, Autilio-Gambetti L, Papasozomenos SC. Bodian's silver method stains neurofilament polypeptides. *Science* 1981; **213**: 1521–1522.

58. Delacourte A, Robitaille Y, Sergeant N *et al.* Specific pathological Tau protein variants characterize Pick's disease. *J Neuropathol Exp Neurol* 1996; **55**: 159–168.
59. Buée L, Delacourte A. Comparative biochemistry of tau in progressive supranuclear palsy, corticobasal degeneration, FTDP-17 and Pick's disease. *Brain Pathol* 1999; **9**: 681–693.
60. Tolnay M, Sergeant N, Ghestem A *et al.* Argyrophilic grain disease and Alzheimer's disease are distinguished by their different distribution of tau protein isoforms. *Acta Neuropathol (Berl)* 2002; **104**: 425–434.

ACADEMIC PRESS

Available online at www.sciencedirect.com

SCIENCE DIRECT®

Neurobiology of Disease 13 (2003) 230–237

Neurobiology of Disease

www.elsevier.com/locate/ynbdi

PML nuclear bodies and neuronal intranuclear inclusion in polyglutamine diseases

Junko Takahashi,[a,b,d,g] Hiroto Fujigasaki,[b] Kiyoshi Iwabuchi,[h] Amalia C Bruni,[i] Toshiki Uchihara,[j] Khalid H. El Hachimi,[c] Giovanni Stevanin,[b] Alexandra Dürr,[b,e,f] Anne-Sophie Lebre,[b] Yvon Trottier,[k] Hugues de Thé,[l] Junichi Tanaka,[g] Jean-Jacques Hauw,[a,d] Charles Duyckaerts,[a,c] and Alexis Brice[b,e,f,*]

[a] *Laboratoire de Neuropathologie Raymond Escourolle, Hôpital de la Salpêtrière, AP-HP, Paris France*
[b] *INSERM U289, Hôpital de la Salpêtrière, AP-HP, Paris, France*
[c] *INSERM U106, Hôpital de la Salpêtrière, AP-HP, Paris, France*
[d] *INSERM U360, Association Claude Bernard, Hôpital de la Salpêtrière, AP-HP, Paris, France*
[e] *Federation de Neurologie, Hôpital de la Salpêtrière, AP-HP, Paris, France*
[f] *Département de Génétique, Cytogénétique et Embryologie, Hôpital de la Salpêtrière, AP-HP, Paris, France*
[g] *Division of Neuropathology, The Jikei University School of Medicine, Tokyo, Japan*
[h] *Department of Neurology and Psychiatry, Kanagawa Rehabilitation Center, Atsugi, Japan*
[i] *Regional Neurogenetic Center, AS6 Lamezia Terme, Italy*
[j] *Department of Neuropathology, Tokyo Metropolitan Institute for Neuroscience, Tokyo, Japan*
[k] *Institut de Génétique, et de Biologie Moléculaire (IGBMC), CNRS, INSERM, Université Louis Pasteur, Illkirch, CU de Strasbourg, France*
[l] *CNRS UPR 9051 Centre Hayem Hôpital, St. Louis, Paris, France*

Received 12 December 2002; revised 12 March 2003; accepted 14 April 2003

Abstract

In polyglutamine diseases, accumulation in the nucleus of mutant proteins induces the formation of neuronal intranuclear inclusions (NIIs). The nucleus is compartmentalized into structural and functional domains, which are involved in NII formation. Promyelocytic leukemia protein (PML), a major component of nuclear bodies, and mSin3A, a component of the transcription co-repressor complex, were used to investigate how the intranuclear domains/sites relate to NII formation in SCA2, SCA3, SCA7, SCA17 and DRPLA brains. We demonstrate that the size of PML-positive intranuclear structures was larger in pathological brains than in control ones and that these structures contained mutant proteins. PML colocalized only with small NIIs, which maintained the ring-like structure of normal nuclear bodies. Enlarged ring-like PML-positive structures, devoid of mutant proteins, were also found and might represent structures where mutant polyglutamine proteins have been successfully processed. These data suggest that NIIs originate from nuclear bodies, where mutant proteins accumulate for degradation.

Keywords: Polyglutamine diseases; Neuronal intranuclear inclusions; Nuclear bodies; Promyelocytic leukemia protein; mSin3A; Ubiquitin; Proteasome

Introduction

Polyglutamine diseases, including spinocerebellar ataxia 1, 2, 3, 6, 7, and 17, Huntington's disease, spinal and bulbar muscular atrophy, and dentatorubral pallidoluysian atrophy (DRPLA) are hereditary neurodegenerative disorders caused by CAG repeat expansions encoding polyglutamine stretches (Fujigasaki et al., 2001; Nakamura et al., 2001; Zoghbi et al., 2000). Although the pathophysiological mechanisms of the polyglutamine diseases still remain to be elucidated, a common pathological hallmark, formation of neuronal intranuclear inclusions (NIIs), may be closely related to their pathogenesis (Ross et al., 1998). NIIs are

* Corresponding author. Pr Alexis Brice, INSERM U 289, Hôpital de la Salpêtrière, AP-HP 47, boulevard de l'Hôpital, 75651 Paris, Cedex 13, France. Fax: +33-1-44-24-36-58.
E-mail address: brice@ccr.jussieu.fr (A. Brice).

0969-9961/03/$ – see front matter © 2003 Elsevier Science (USA). All rights reserved.
doi:10.1016/S0969-9961(03)-00080-9

ubiquitinated and contain proteosomal subunits, indicating that the NIIs are formed when misfolded mutant proteins are degraded through the ubiquitin-proteosome pathway (Chai et al., 1999; Cummings et al., 1998; Stenoien et al., 1999; Wyttenbach et al., 2000). NII formation takes place in the nucleus, and several nuclear proteins, such as transcription regulators, have been detected in the NIIs (Boutell et al., 1999; McCampbell et al., 2000; Shimohata et al., 2000; Wood et al., 2000). These nuclear proteins are often compartmentalized into organized structural and functional domains (Dundr et al., 2001). Recent studies have shown that polyglutamine proteins are associated with these functional intranuclear structures, which might therefore be involved in NII formation. One of the most important intranuclear structures, referred to as "nuclear bodies" (NBs), is distributed throughout the nucleus with a speckled pattern. Although the function of the NBs remains unknown, they have been proposed to be involved in many cellular processes, such as transcriptional regulation, growth suppression and apoptotic cell death (Seeler et al., 1999; Zhong et al., 2000). Promyelocytic leukemia protein (PML), an essential component of NBs, has been shown to localize to NIIs in both in vitro and in vivo studies. When mutant ataxin-1 induces the formation of nuclear aggregates in cellular models, PML redistributes to the aggregates (Skinner et al., 1997) and mutant ataxin-3 and mutant ataxin-7 colocalize with PML in transfected cells (Chai et al., 1999; Kaytor et al., 1999; Tait et al., 1998). In human brains, NIIs observed in SCA3, SCA7 and DRPLA are colocalized with PML in a characteristic pattern. Yamada et al. have shown that when there are several NIIs in a neuron, PML is found in only one of them (Yamada et al., 2001a; Yamada et al., 2001b). Our previous study on SCA7 brains demonstrated that only small NIIs contain PML (Takahashi et al., 2002). This observation suggests that NBs accumulate ataxin-7 and form small NIIs that gradually lose their characteristic features as the mutant polyglutamine-containing protein accumulates and the size of the NIIs increases. Recent studies showing that NBs are associated with the ubiquitin proteasome pathway and might be sites of protein degradation in nuclei (Everett et al., 1997; Lallemand Breitenbach et al., 2001; Mattsson et al., 2001; Reyes, 2001) suggest that NB could be involved in the processing of pathological polyglutamine proteins.

Several transcription factors and co-factors, which are compartmentalized into intranuclear domains/sites, are recruited into NIIs. GREB-binding protein (CBP), a transient component of NBs, is entrapped in NIIs (Nucifora et al., 2001; Shimohata et al., 2000). The transcription co-repressor mSin3A, which forms a complex of repressor proteins including the N-terminal region of the nuclear receptor co-repressor (N-CoR) and histone deacetylases (Boutell et al., 1999), is recruited into a subset of NIIs of Huntington's disease. Since N-CoR potentially interacts with huntingtin (Boutell et al., 1999), its recruitment into NII could occur through the formation of the co-repressor complex, suggesting that the nuclear domains containing transcription co-repressors are also involved in the process of NII formation.

Table 1
Summary of clinical findings of the patients

		Gender	Age at onset	Age at death
SCA2	Patient 1	M	30	50
	Patient 2	F	27	48
	Patient 3	M	47	57
SCA3	Patient 4	F	42	64
	Patient 5	M	22	36
	Patient 6	F	25	42
	Patient 7	F	27	40
	Patient 8	F	37	51
SCA7	Patient 9	M	5	10
SCA17	Patient 10	F	17	49
DRPLA	Patient 11	F	4	24
	Patient 12	F	33	46

In this study, we examined autopsied brains of SCA2, SCA3, SCA7, SCA17 and DRPLA cases and extended our previous results obtained on SCA7 brains showing that PML/NBs are commonly associated with NII formation in a size-dependent manner in the 5 types of polyglutamine disease. We also found that recruitment of mSin3A into NIIs was common to all of the polyglutamine diseases examined, but with different frequencies. We discuss how the two different intranuclear domains/sites, NBs and transcription co-repressor complexes, relate to the formation of NIIs in different types of polyglutamine disease.

Patients and methods

Brains obtained at autopsy from 3 patients with SCA2, 5 patients with SCA3, 1 patient with SCA7, 1 patient with SCA17, 2 patients with DRPLA and 5 controls (aged 27 to 93; mean, 64.0) were available for this study. Clinical findings in the patients were summarized in Table 1. All of them died from pneumonia.

Immunohistochemistry

Formalin-fixed paraffin-embedded blocks of the pontine nucleus of all cases and frontal cortex of the SCA17 case were cut and used for immunohistochemical staining. Since NIIs were very rare in the pontine nucleus of the SCA17 patient, sections of frontal cortex were used for quantitative analysis. The following antibodies were used: anti-ataxin-2 (dilution 1:100, mouse monoclonal clone 15F6, IgM class: Imochem, Christchurch, New Zealand), anti-ataxin-3 (dilution 1:1,000, rabbit polyclonal) (Fujigasaki et al., 2000), anti-ataxin-7 1C1 (dilution 1:10,000, mouse monoclonal)

(Yvert et al., 2000), anti-TATA box binding protein (TBP) (dilution 1:500, rabbit polyclonal, Santa Cruz Biothech, Santa Cruz, CA, USA), anti-atrophin-1 (dilution, USA 1:800, goat polyclonal) (a gift from Dr. CA Ross, Johns Hopkins University School of Medicine, Baltimore, USA), anti-polyglutamine 1C2 (dilution 1:8,000, mouse monoclonal, USA Chemicon, Temecula, CA, USA), anti-PML (dilution 1:200, chicken polyclonal) (Daniel et al., 1993), anti-mSin3A (AK-11) (dilution 1:200, rabbit polyclonal, Santa Cruz Biothech, Santa Cruz, CA, USA). To expose the antigenic epitopes, sections were autoclaved in 10 mM citrate buffer (pH 6.0) for 10 min and immersed in 1% periodic acid for 15 min. If necessary, they were then immersed in 99% formic acid for 5 min. After the pretreatment, the sections were incubated with one of the primary antibodies, then with biotinylated secondary antibodies and horseradish peroxidase conjugated streptavidin. Diaminobenzidine was used as the chromogen (DAKO ChemoMate Detection kit, DAKO, Glostrup, Denmark).

The size of intranuclear aggregates/structures stained with anti-PML and 1C2 antibodies were measured as previously described (Takahashi et al., 2002). Microscopic fields (×1000 magnification) of the immunostained sections were visualized on a monitor. The long axes of NIIs were plotted manually and measured automatically with an image analyser (VisioScan Biocom, Les Ulis, France). Aggregates smaller than 0.5 μm were excluded from this analysis. In SCA3 and SCA7 cases, 50 intranuclear aggregates stained with the anti-PML and 1C2 antibodies were examined in each section. In SCA2, SCA17 and DRPLA cases, 20 aggregates were examined. Differences between the sizes of the immunopositive intranuclear aggregates labelled by the anti-PML and the 1C2 antibodies were evaluated by non-parametric analysis using the Mann-Whitney test. To estimate the maximum size of normal NBs, the size of PML-immunoreactive intranuclear structures was determined in 200 neurons in each normal control case.

Double immunofluorescent labelling was performed to examine the colocalization of mutant polyglutamine proteins (revealed by 1C2) with PML. The secondary antibodies were anti-mouse IgG or anti-chicken IgG antibodies coupled with FITC (emission peak 525 nm) (Amrad Biotech, Victoria, Australia) or with Cy3 (emission peak 568 nm) (Jackson Immunoresearch, West Grove, PA). The slides were examined with a Leica TCS 4D confocal microscope. 1C2- or PML-immunopositive intranuclear aggregates/structures were examined in the double immunostained sections to estimate the frequency of colocalization of these two proteins in the same structures. In this analysis, first, PML immunoreactive ring-like structures (≥0.5 μm) were detected and their immunoreactivity to 1C2 was examined. Then, unambiguous 1C2-immunoreactive intranuclear aggregates (≥0.5 μm) were identified and their immunoreactivity to PML was examined. Ten (SCA2, SCA3 and DRPLA) or twenty (SCA7 and SCA17) 1C2- or PML-immunopositive intranuclear aggregates/structures were examined in each case.

Consecutive sections stained with anti-mSin3A and the 1C2 antibodies were used to estimate frequency of mSin3A immunopositive NIIs. Microscopic fields (×400 magnification) of each section were displayed on the monitor as described above. The total number of neurons and the number of neurons containing-unambiguous NIIs were counted until at least 200 neurons were encountered. When the frequency of NIIs stained with at least one of the two antibodies was less than 1%, counting was continued until at least 500 neurons were examined. The number of unlabelled neurons and of neurons containing inclusions labelled with anti-mSin3A or the 1C2 antibody was tabulated in a contingency table. The difference between the number of neurons immunolabelled with anti-mSin3A and the 1C2 antibody was tested using Fisher's exact test.

Results

Distribution of the proteins in control cases

In normal neurons, ataxin2-like immunoreactivity (IR) was found in both nuclei and cytoplasm. Ataxin3-like IR was granular and mainly found in the cell body of the neurons. Ataxin-7 was found in cell bodies and sometimes in nuclei of neurons. Fine granular TBP-like IR was detected mainly in the cytoplasm of neurons. Atrophin-1-like IR was finely granular in normal neuronal nuclei. No obvious staining by the 1C2 antibody was found in normal neurons. The nucleus of the neurons contained several (5 to 15) small PML-immunoreactive dots, which corresponded to NBs. The maximum size of PML-immunoreactive intranuclear structures in the 5 normal control cases ranged from 0.62 to 0.83 μm (mean 0.73 μm). The mSin3A immunoreactivity was found mainly in the cytoplasm of the neurons. Diffuse or granular nuclear staining was observed in only a few neurons.

NIIs in SCA2, SCA3, SCA7, SCA17 and DRPLA

NIIs labelled with the 1C2 antibody and antibodies directed against the corresponding polyglutamine proteins (ataxin-2, 3, 7, TBP, atrophin-1) were found in all cases. Although NIIs from each case were immunoreactive for ataxin-2, 3, TBP and atrophin-1, ataxin-7 was found only in NIIs from the SCA7 case.

Sizes of PML and 1C2 immunoreactive intranuclear aggregates

Our previous study in the cerebral cortex of SCA7 patients demonstrated that PML is preferentially found in small NIIs (Takahashi et al., 2002). We therefore determined the size distribution of aggregates labelled by the

Table 2
Size of the 1C2 and PML positive intranuclear aggregates/structures

		Sizes of intranuclear aggregates/structures (mm)					
		1C2			PML		
		Min	Max	Mean	Min	Max	Mean
SCA2	Patient 1*	1.1	3.6	2.5	0.78	2.6	1.3
	Patient 2*	1	4.1	2.5	0.84	2.2	1.3
	Patient 3*	0.86	4.6	2.8	0.63	2.6	1.4
SCA3	Patient 4*	0.9	4.1	2	0.5	2.5	1.3
	Patient 5*	0.82	3.7	1.9	0.78	2.2	1.5
	Patient 6*	0.85	4.6	1.8	0.85	2	1.5
	Patient 7*	0.82	4.1	2	0.8	2.9	1.6
	Patient 8*	0.82	3.6	2	0.9	2.3	1.5
SCA7	Patient 9*	0.57	4.3	2.3	0.64	2.9	1.2
SCA17	Patient 10*	1.3	3.2	2.2	1	2.4	1.5
DRPLA	Patient 11*	1.2	3.1	2	1.2	3.1	1.9
	Patient 12**	1.2	3.7	2.1	1	3.2	1.9

Non-parametric analysis using the Mann-Whitney test showed that the size of intranuclear aggregates/structures detected by the anti-PML antibody was significantly smaller than those detected by the 1C2 antibody (*$p < 0.001$, **$p < 0.02$). Aggregates smaller than 0.5 mm were excluded from this analysis.

anti-PML and 1C2 antibodies in other polyglutamine diseases to see whether PML showed the same distribution as in SCA7 (Table 2). In all cases examined, some neurons contained large PML-immunopositive structures (>1.0 μm), which were not observed in normal control cases. The maximum size of these structures found in SCA2, SCA3, SCA7, SCA17 and DRPLA was 2.6, 2.9, 2.9, 2.4 and 3.2 μm, respectively. In contrast, the maximum size of the NIIs visualized by the 1C2 antibody was 4.6, 4.6, 4.3, 3.2, and 3.7 μm in SCA2, SCA3, SCA7, SCA17 and DRPLA, respectively. The size of intranuclear aggregates/structures detected by the anti-PML antibody was significantly smaller than that detected by the 1C2 antibody in all the cases examined except one case with DRPLA. Although structures detected by the 1C2 and the anti-PML antibodies were not always colocalized as described in the next section, the significant difference in size suggests that PML is rarely associated with large NIIs.

Colocalization of PML and expanded polyglutamine

Images obtained by confocal microscopy demonstrated that PML-like IR was found in only a subset of NIIs (Table 3, left half column) and frequently in small NIIs (Fig. 1, A–C and D–F). In the NIIs, PML-IR was often accentuated at the periphery of the structures and showed the ring-like appearance previously reported in SCA3, SCA7 and DRPLA (Fig 1, B, E and H). However, these large PML ring-like structures did not always contain the 1C2 epitope (Fig 1, G–I) and the frequency of colocalization varied among cases (Table 3, right half column). Although the number of cases examined in each disease was limited, there was a tendency for the frequency of co-localization to vary according to the type of diseases. In all SCA3 cases, the frequency of PML positive structures containing the 1C2 epitope was high. In contrast, ≤50% of them were co-localized with the 1C2 epitope in SCA2 cases.

Frequency of mSin3A positive NIIs

NIIs positive for mSin3A were found in SCA2, SCA3, SCA7, SCA17 and DRPLA brains. To assess the frequency of NIIs containing mSin3A, sections stained with the anti-mSin3A and 1C2 antibodies were examined. mSin3A was preferentially recruited into NIIs in DRPLA (Table 4) (Fig. 1, J and K). In SCA2, SCA3 and SCA7 cases, there were significantly fewer mSin3A- than 1C2-immunopositive NIIs. In SCA17, the frequency of NIIs was too low to be statistically significant ($p = 0.064$).

Discussion

In all polyglutamine diseases examined in this study, PML-immunopositive intranuclear structures were larger than in controls. Indeed, NBs in controls are mostly ≤1 μm in size, whereas the mean size of PML-positive structures was greater than 1.2 μm in all cases. In addition, a variable proportion of PML containing structures colocalize to NII, which contain abnormal polyglutamine protein, suggesting that NBs are associated with NII formation in the 5 types of polyglutamine disease examined. As NIIs observed in polyglutamine diseases are ubiquitinated and contain proteasome subunits, it has been proposed that NII formation represents a cellular reaction to reduce polyglutamine toxicity, possibly through the ubiquitin proteasome protein

Table 3
Frequency of co-localization of 1C2 and PML in intranuclear aggregates/structures

		1C2-positive aggregates	PML-positive structures
		PML(+)	1C2(+)
SCA2	Patient 1	2/10	2/10
	Patient 2	1/10	4/10
	Patient 3	1/10	5/10
SCA3	Patient 4	7/10	10/10
	Patient 5	6/10	10/10
	Patient 6	7/10	10/10
	Patient 7	4/10	9/10
	Patient 8	5/10	10/10
SCA7	Patient 9	6/20	17/20
SCA17	Patient 10	3/20	2/20
DRPLA	Patient 11	3/10	8/10
	Patient 12	6/10	7/10

First, 1C2-positive intranuclear aggregates were detected and their immunoreactivity to PML was examined (left column). Then, PML-positive intranuclear structures were detected and their immunoreactivity to 1C2 was examined (right column). +strongly immunoreactive.

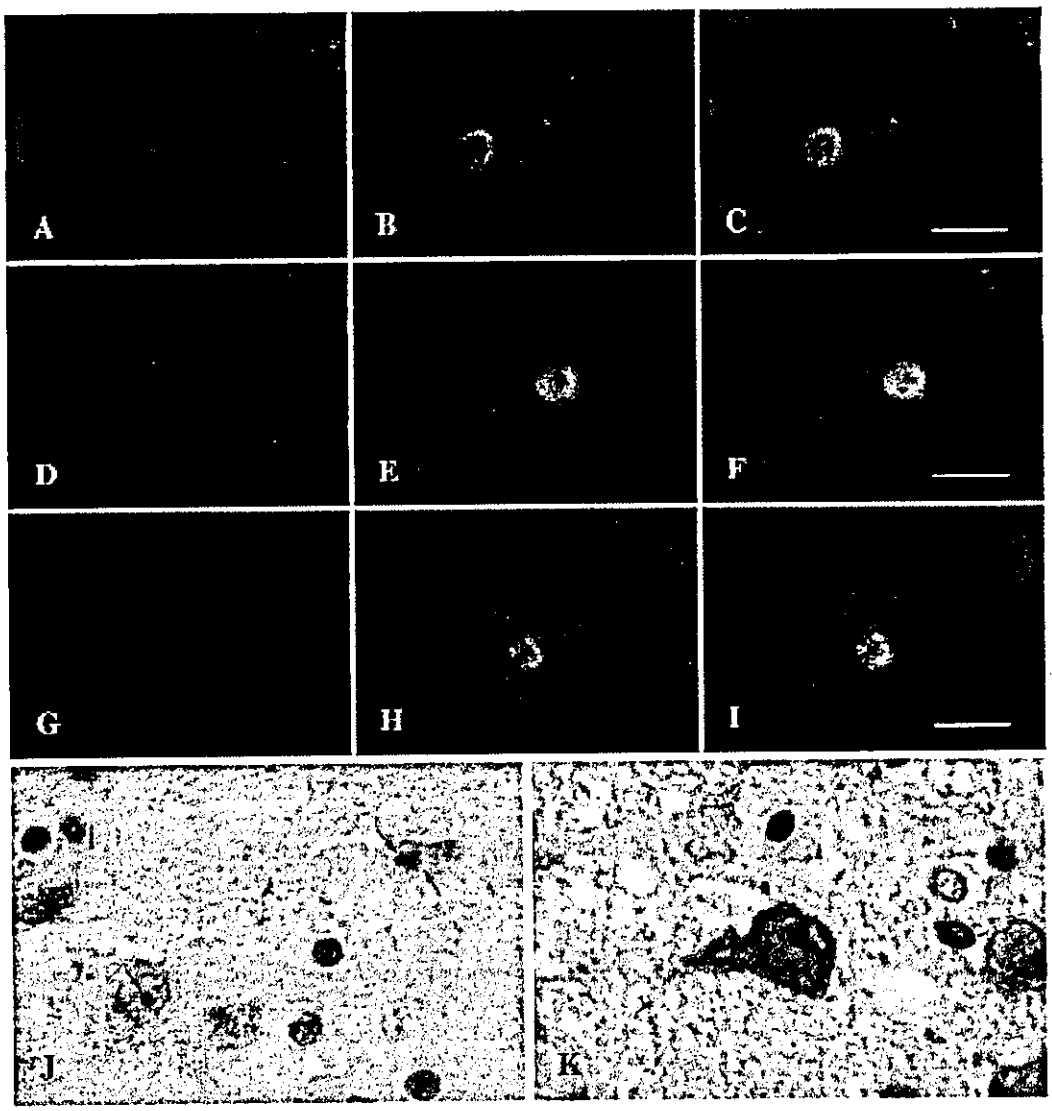

Fig. 1. (A–I) Double labelling with antibodies against polyglutamine (1C2) and PML. (A,D,G: 1C2, B, E, H: PML, C, F, I: merged.). In SCA2 (A–C: pontine nucleus) and SCA3 (D–F: pontine nucleus) brains, only the smaller of the two NIIs was colocalized with PML. Note that PML surrounded the 1C2-immunopositive NIIs, in a ring-like structure. Large ring-like PML-positive structures did not contain the 1C2 epitope, in the SCA17 brain (G–I: frontal cortex). (J, K) mSin3A immunolabelling in DRPLA (J: pontine nucleus) and SCA7 (K: pontine nucleus) brains. mSin3A immunoreactive NIIs were frequently observed in DRPLA (arrows). In SCA7, mSin3A immunoreactive NIIs were rare. Note that NII remained unstained by anti-mSin3A antibody (arrow).

degradation pathway (Cummings et al., 1999; Klement et al., 1998; Kuemmerle et al., 1999; Saudou et al., 1998). Recent studies have shown that NBs might also serve as sites for protein degradation in nuclei. Anton et al. demonstrated that mutant forms of influenza virus nucleoprotein accumulate in NBs, when treated with proteasome inhibitors (Anton et al., 1999). Considering that PML is a RING finger protein, which is proposed to act as a E3 ubiquitin ligase (Freemont, 2000; Reyes, 2001), it could be involved in the degradation of abnormal polyglutamine proteins through formation of NII. In a previous study using SCA7 brains, we have demonstrated that PML is preferentially found in small NIIs but is excluded from large ones (Takahashi et al., 2002). A process of NII formation has been proposed, in which NBs are gradually enriched in mutant proteins and finally lose their characteristic structure, as the accumulation of mutant proteins enlarges them. In this study, we confirm that PML is also associated with NIIs in a size-dependent manner in 4 other types of polyglutamine disease.

PML-like immunoreactivity was often accentuated at the periphery of NIIs in a ring-like structure, suggesting an alternative hypothesis: PML is redistributed around NIIs (Skinner et al., 1997; Yamada et al., 2001a). In normal cells, PML is also found at the margin of "mature NBs", with a similar ring-like distribution (Zhu et al., 2001). There is

Table 4
Frequency of 1C2- and mSin3A-immunopositive intranuclear aggregates

		Frequency of intranuclear aggregates	
		1C2	mSin3A
SCA2	Patient 1*	5.9%	<1%
	Patient 2**	3.6%	<1%
	Patient 3*	3.5%	0%
SCA3	Patient 4*	14.2%	1.4%
	Patient 5*	43.0%	4.4%
	Patient 6*	43.6%	10.2%
	Patient 7*	31.4%	7.6%
	Patient 8*	46.0%	6.8%
SCA7	Patient 9*	10.2%	1.8%
SCA17	Patient 10	1.2%	<1%
DRPLA	Patient 11	1.6%	2.4%
	Patient 12	3.1%	4.4%

The frequency of mSin3A-positive aggregates was significantly lower than 1C2-positive aggregates (*$p < 0.005$, **$p < 0.05$).

evidence that PML itself can be degraded in mature NBs, which recruit proteasome subunits (Zhu et al., 2001). Although how the ring-like structures containing PML are formed in polyglutamine diseases has not been elucidated, one might postulate that they correspond to enlarged NBs that have accumulated abnormal polyglutamine proteins for degradation. Some of these ring-like PML-positive structures did not contain the 1C2 epitope, and may be considered to be "empty large NBs". These structures may be NBs in which the polyglutamine proteins have already been processed, so that the 1C2 epitopes would already have been degraded. Although the number of cases examined was limited, the proportion of "empty large NBs" seemed, at least in part, dependent on the type of disease. They were quite rare in the SCA3 cases, compared with other types of polyglutamine diseases examined, indicating that the nature of the polyglutamine protein itself might be one of determinants. A recent study has shown that ataxin-3 interacts directly or indirectly with PML and CBP, both of which are components of NBs that potentially form multiprotein complexes (Chai et al., 2001). Formation of the multiprotein complexes might stabilize ataxin-3 in NBs, resulting in a low frequency of "empty large NBs". In the SCA3 cases with a low frequency of "empty large NBs" (0/10 or 1/10), the population of 1C2 positive NIIs was greater (14.2 to 46.0%) than in the other types of polyglutamine diseases (1.2 to 10.2%). This result shows that more NIIs are present when the NBs are full of mutant protein. This observation also supports our hypothesis that NIIs originate from enlarged NBs that accumulate mutant polyglutamine proteins.

It is a matter of discussion how the structural changes of NBs relate to pathogenesis. A number of recent studies on polyglutamine diseases showed that impaired transcription might be responsible for neuronal dysfunction, which precedes overt neuronal cell death (McCampbell et al., 2000; Nucifora et al., 2001; Shimohata et al., 2001; Steffan et al., 2000). NBs contain some molecules, such as CBP, p53 and sp100 that regulate transcription and cell growth (Zhong et al., 2000). Disruption of the integrity of normal NBs could therefore result in deregulation of transcription and finally in neuronal death.

We have also found that mSin3A, a transcription co-repressor, is frequently associated with NIIs in DRPLA. Atrophin-1, the DRPLA gene product is functionally related to transcription co-repressors and their complexes. Atrophin-1 interacts with ETO/MTG8, a component of nuclear receptor co-repressor complexes. Atrophin-1 and ETO/MTG8 colocalizes with intranuclear structures containing mSin3A and histone deacetylases in a cellular model of DRPLA (Wood et al., 2000). In addition, a recent study using a *Drosophila* model has shown that atrophin-1 can function as a transcription co-repressor and that deregulation of transcription may contribute to the pathogenesis of DRPLA (Zhang et al., 2002). The normal function of atrophin-1 could, therefore, be implicated in the frequent localization of mSin3A in NIIs in DRPLA. mSin3A was also found in NIIs formed in other polyglutamine diseases. Since PML interacts with multiple co-repressors containing mSin3A, N-CoR and histone deacetylase (Khan et al., 2001), this might account for the accumulation of mSin3A in NIIs, which probably originate from NBs.

In conclusion, this study suggests that NIIs in polyglutamine diseases could originate from NBs, which are significantly enlarged in these conditions. When excessive accumulation of mutant proteins destroys the structure of NBs, large NIIs that contain little or no PML are formed. In contrast, "empty large NBs" might represent structures in which polyglutamine proteins have been successfully processed, explaining why no 1C2 immunoreactivity is detected. This interpretation of the morphological data, consistent across the 5 polyglutamine diseases studied, is supported by accumulating evidence that NB could be involved in protein processing. This hypothesis opens new pathways for investigating the mechanisms of neuronal degeneration in polyglutamine diseases.

Acknowledgments

We thank Dr. CA Ross for the kind gift of the anti-Atrophin-1 antibody, Dr. M. Ruberg for critical reading of the manuscript and Ms. K. Yamaoka for technical assistance. This work was jointly supported by INSERM and the Japan Society for the Promotion of Science (J.T., K.I., T.U., and C.D.) and by the VERUM Foundation. J.T. was supported by a fellowship from Association of Claude Bernard and H. F. by a fellowship from EGIDE.

References

Anton, L.C., Schubert, U., Bacik, I., Princiotta, M.F., Wearsch, P.A., Gibbs, J., Day, P.M., Realini, C., Rechsteiner, M.C., Bennink, J.R.,